Floquet states of a kicked particle in a singular potential: Exponential and power-law profiles

Sanku Paul* and M. S. Santhanam†
Indian Institute of Science Education and Research, Dr. Homi Bhabha Road, Pune 411 008, India

(Received 19 December 2017; published 27 March 2018)

It is well known that, in the chaotic regime, all the Floquet states of kicked rotor system display an exponential profile resulting from dynamical localization. If the kicked rotor is placed in an additional stationary infinite potential well, its Floquet states display power-law profile. It has also been suggested in general that the Floquet states of periodically kicked systems with singularities in the potential would have power-law profile. In this work, we study the Floquet states of a kicked particle in *finite* potential barrier. By varying the height of finite potential barrier, the nature of transition in the Floquet state from exponential to power-law decay profile is studied. We map this system to a tight-binding model and show that the nature of decay profile depends on energy band spanned by the Floquet states (in unperturbed basis) relative to the potential height. This property can also be inferred from the statistics of Floquet eigenvalues and eigenvectors. This leads to an unusual scenario in which the level spacing distribution, as a window in to the spectral correlations, is not a unique characteristic for the entire system.

DOI: 10.1103/PhysRevE.97.032217

I. INTRODUCTION

Dynamical localization of Floquet states in time-dependent and chaotic Hamiltonian systems is a phase coherent effect arising from quantum interferences. Quantum kicked rotor is a paradigmatic model for quantized chaotic systems that displays localization effects. Quantum localization in kicked rotor (KR) continues to attract attention in a variety of contexts ranging from metal-insulator transitions [1,2], coherent control [3], entanglement measures [4], quantum resonances [5–8], quantum ratchets [9,10], to quantum transport [11] and decoherence effects [12,13]. Most of such studies have focused on KR as a model for time-dependent potential exhibiting classically chaotic dynamics and quantum mechanical localization. For sufficiently strong nonlinearity, KR displays chaotic classical dynamics and it is associated with diffusive growth of mean energy with time. In the corresponding quantum regime, this unbounded energy growth is strongly suppressed by localization arising from destructive quantum interferences [14]. This effect in KR has been shown to be analogous to Anderson localization for electronic transport in crystalline solids [15–17].

One significant property shared by the quantum KR and Anderson model is the exponential decay of their eigenstates. In the one-dimensional Anderson model all the eigenstates are exponentially localized in position representation [18,19], i.e., $\psi(x) \sim e^{-x/x_l}$, where x_l is the localization length. In the KR system, eigenstates are exponentially localized in the momentum representation [20]. The latter has been experimentally realized in microwave ionization of hydrogen atoms and in cold atomic cloud in optical lattices [21–23].

Kicked rotor can thus be regarded as a representative dynamical system from two distinct points of view. First, in the classical sense, it belongs to a class of chaotic systems that obeys Kolmogorov-Arnold-Moser (KAM) theorem [24]. This effectively implies that, upon variation of a chaos parameter, the system makes a smooth transition from regular to predominantly chaotic dynamics. Second, in the quantum mechanical regime, KR is a paradigmatic example of dynamical localization and the associated exponential profile of its Floquet states. In the past decade, many other facets of chaos and localization in variants of KR have been studied that have provided results different from this standard scenario [2,25–28].

One class of important variant is to place the KR in a singular potential. Presence of singularity in the potential violates one of the conditions for the applicability of KAM theorem and leads to a scenario in which abrupt, rather than smooth, transition from integrability to chaotic dynamics becomes possible. Such abrupt transition to chaos is a feature of non-KAM systems and is seen, for instance, in the kicked particle in an infinite potential well [29,30]. The quantum eigenstates of this system had been reported to display localization and its profile is *not* exponential but was claimed to have power-law-type decay in the unperturbed basis. A more systematic study in Ref. [2] incorporated singularity in the KR through a tunable potential term $V(q;\alpha)$ such that it becomes singular at some special value of tunable parameter $\alpha = \alpha_s$. It was shown, through numerical simulations, that if $\alpha = \alpha_s$ in the potential, then all the eigenstates of the system are power-law localized. Indeed, it was even suggested that KR when acted upon by a singular potential would display eigenstate localization with power-law profile in contrast to the exponential profile obtained in the context of standard KR [30,31]. This suggestion has not yet been numerically tested in a variety of chaotic Hamiltonian systems and general analytical results in support for this claim remains an open question.

*sankup005@gmail.com
†santh@iiserpune.ac.in

A related question is that of the spectral statistics of systems with singular potentials. Many earlier results have shown that Hamiltonians with singular potentials display "critical" statistics characterized by (i) level spacing distribution that lies intermediate between the Wigner and Poisson limits and (ii) multifractal eigenvector statistics. Interestingly, this is also the statistical signature of the Anderson model in more than two dimensions at the metal-insulator transition [32]. In the case of a kicked rotor system with a steplike singular potential, it was shown that the level spacings s follow semi-Poisson distribution $P(s) = 4se^{-2s}$ [33] and eigenfunctions exhibit a nontrivial scaling of moments, a manifestation of its multifractal nature [2]. Similar spectral statistics occurs for the case of disordered Hamiltonians with nonanalytic dispersion relation [34], in a near-integrable generalized kicked rotor with a smooth potential [27] and in quantum maps which are classically pseudointegrable [35].

In this paper, we examine the question whether the presence of nonanalytic potential in a kicked rotor would *generically* imply power-law profile and other signatures of critical statistics for its eigenstates in the quantum regime. To address these questions, we consider the dynamics of a periodically kicked particle placed in a stationary finite potential well of height V_0. This is primarily a non-KAM system and its unusual classical and quantum transport properties, reflective of its non-KAM nature, were recently reported in Ref. [36]. This system subsumes two limiting cases: it is the standard KR (a KAM system) in the absence of finite well potential, i.e., $V_0 = 0$ and if $V_0 \to \infty$, then it becomes a kicked rotor system placed in an infinite well (a non-KAM system) and has been studied in Refs. [29,30]. Hence, this is a suitable test bed to understand the transition in the nature of Floquet states as V_0 is varied from the limit of a KR system (analytic potential) to that of a system with singular potential. Further, this can lead to a better understanding of the quantum manifestations of classical chaos non-KAM systems.

Using the context of this system based on KR, we show in this paper that the presence of singularity in the potential does not always guarantee power-law localization of Floquet states. It must be noted that in contrast to Ref. [2], in which potential can be tuned for singularity, in the present case the potential always displays singularity. Singular potentials are associated with power-law localized Floquet states provided that the Floquet states span an energy band in which the singularity is effectively felt by the particle. Further, it is demonstrated that the spectral fluctuations properties such as the level spacing distributions for this system depends on the energy range being considered. Hence, spacing distributions do not characterize the system at all the energy scales.

In Sec. II, we introduce the model of kicked particle in a finite barrier. In Sec. III, we report results on the decay profile of the Floquet states and relate it to the decay of the Floquet matrix and to the effective singularity "felt" by the kicked particle at various energy scales. In Sec. IV, we obtain a tight-binding form for our system to deduce the nonexponential nature of Floquet state decays. Finally, in Sec. V, we discuss the manifestation of potential singularity in the averaged quantities derived from Floquet states.

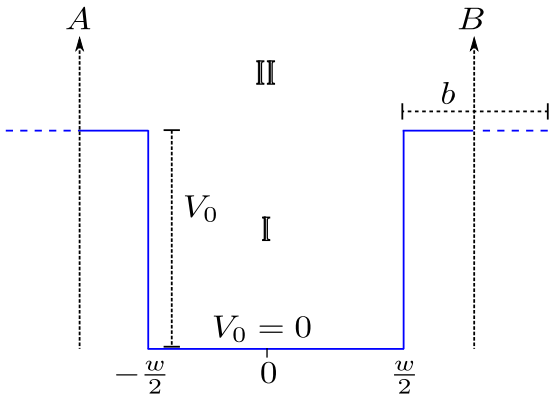

FIG. 1. Schematic of the stationary potential, $V_{sq}(\theta)$ with V_0 as the potential height, b and w as barrier and well width, respectively. A and B represent the positions at which periodic boundary conditions are applied. I and II denotes the regions below and above V_0.

II. KICKED PARTICLE IN FINITE BARRIER

The dimensionless Hamiltonian of a periodically kicked particle in a finite well potential [36] is

$$H = \frac{p^2}{2} + V_{sq}(\theta) + k\cos(\theta)\sum_{n=-\infty}^{\infty}\delta(t-n)$$
$$= H_0 + V(\theta)\sum_{n=-\infty}^{\infty}\delta(t-n). \quad (1)$$

In this, $V(\theta) = k\cos(\theta)$ and $V_{sq}(\theta)$ is the square well potential shown in Fig. 1 and can be represented as

$$V_{sq}(\theta) = V_0[\Theta(\theta - R\pi) - \Theta(\theta - R\pi - b)],$$

where V_0 is the potential height and b is the barrier width, $R = w/\lambda$ is the ratio of well width to the wavelength of the kicking field, and k is the kick strength. Throughout this work, we have set $\lambda = 2\pi$, b, and w are constrained by $b + w = 2\pi$. Periodic boundary conditions are applied at positions A and B shown in Fig. 1.

Let E_n and $|\psi_n\rangle$ represent the energy and the eigenstate of the unperturbed system such that $H_0|\psi_n\rangle = E_n|\psi_n\rangle$. Further, $|\psi_n\rangle$ can be written as a superposition of all momentum states $|l\rangle$, i.e., $|\psi_n\rangle = \sum_l a_{nl}|l\rangle$, where a_{nl} represents the expansion coefficient. Then any general initial state can be expressed in the energy basis state representation as $|\Psi\rangle = \sum_n b_n|\psi_n\rangle$. The mean energy in the state $|\Psi(t)\rangle$ can be obtained as

$$E(t) = \langle\Psi(t)|\hat{H}_0|\Psi(t)\rangle$$
$$= \sum_m E_m|b_m(t)|^2. \quad (2)$$

The quantum map that connects the state $|\Psi(N+1)\rangle$ at time $N+1$ with the state $|\Psi(N)\rangle$ can be obtained by evolving the Schroedinger equation $|\Psi(N+1)\rangle = \widehat{U}|\Psi(N)\rangle$, where $\widehat{U}$ is the Floquet operator,

$$\widehat{U} = e^{-H_0/\hbar_s}e^{-iV(\theta)/\hbar_s}, \quad (3)$$

and $\hbar_s$ is the scaled Planck's constant. In the energy representation, the elements of the Floquet operator are given by

$$U_{nm} = \sum_{p,p'} a^*_{np} a_{mp'} i^{|p-p'|} J_{|p-p'|}\left(\frac{k}{\hbar_s}\right), \tag{4}$$

where $J_{|p-p'|}(\cdot)$ is the Bessel function of order $|p-p'|$.

The eigenvalue equation governing the Floquet operator is $\widehat{U}|\phi\rangle = e^{i\omega}|\phi\rangle$ in which $|\phi\rangle$ represents a Floquet state and ω is its quasienergy. The Floquet operator is a unitary operator and hence the eigenvalues lie on a unit circle. Further the quasienergy state, $|\phi\rangle$, can be decomposed as a superposition of all energy states $|\psi_n\rangle$, i.e., $|\phi\rangle = \sum_n c_n|\psi_n\rangle$, where $|c_n|$ is the probability density of finding the particle in state $|\psi_n\rangle$.

To analyze the localization properties of the Floquet states, Floquet matrix of order N is numerically diagonalized to determine the quasienergies and the Floquet vectors. In this work, $N = 10\,035$ and we have ensured that for the choice of parameters used in this paper, the system is classically chaotic (see Appendix A). Floquet states for standard KR are generally known to be exponentially localized in momentum space $|\psi(p)|^2 \sim \exp(-p/\xi)$ characterized by a localization length ξ. In contrast to that, Floquet states of a kicked particle in a periodic potential well is localized over energy basis state $|\psi_n\rangle, n = 1,2,\ldots$. In the subsequent sections, it is shown that the system in Eq. (1) exhibits a transition from exponential to power-law localization as the parameters V_0 and k are varied.

III. FLOQUET STATES

In this section, we will mainly focus on the average spectral properties of the Floquet states which governs the dynamics in the quantum regime. For the finite well represented by Hamiltonian in Eq. (1), the nature of Floquet state decay profile, in general, will depend on the choice of parameters, namely, kick strength k and potential height V_0. Figure 2 has been obtained by averaging over 10 035 Floquet states $|\phi\rangle(= \sum_n c_n|\psi_n\rangle)$ for each set of parameters. Prior to averaging, each Floquet state was shifted by $n_{\max}$, i.e., $v = n - n_{\max}$, where $n_{\max}$ corresponds to n for which $|c_n|^2$ is maximum.

If $V_0 > 0$, the Hamiltonian in Eq. (1) is a non-KAM system due to the presence of singularities in $V_{\text{sq}}(\theta)$. Based on numerical simulations of kicked systems with singular potentials, it was argued that their Floquet states display power-law decay over the unperturbed basis [2,29–31,37]. Further, a new universality class has been proposed in Ref. [2] based on the presence of classical singularity and power-law localization. To discuss the results, in the light of this proposal, two limiting cases can be identified; (i) $0 < V_0 < 1$ (KR limit) and (ii) $V_0 \gg 1$ [KR in infinite well (KRIW) limit]. In the KR limit, notwithstanding the singularity in the potential, the Floquet states can be expected to be qualitatively closer to that of KR. In particular, if kick strength $k \gg 1$, all the Floquet states display exponential decay profile. On the other hand, in the KRIW limit, the potential height is large ($V_0 \gg 1$) and is qualitatively closer to the kicked infinite well system [29,30]. In this limit, even for small kick strengths $k < 1$, it is known that all the Floquet states show power-law decay over the unperturbed basis [30,31]. Both these limits are illustrated in Fig. 2.

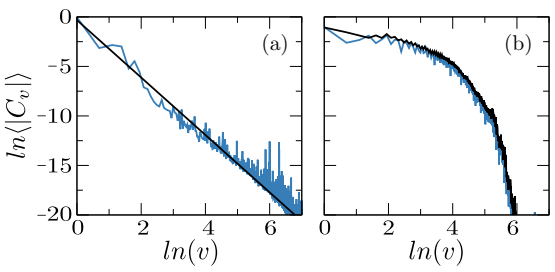

FIG. 2. Decay of Floquet states over the unperturbed basis states, averaged over all the Floquet states. The parameters are $b = 1.4\pi, \hbar_s = 1.0$, (a) (KRIW limit) $V_0 = 5000.0, k = 0.25$, and (b) (KR limit) $V_0 = 0.5, k = 4.25$. In (a) the black line is a linear fit and in (b) the black curve corresponds to KR.

In Fig. 2(a), the decay of the averaged Floquet state in the KRIW limit is shown for $V_0 = 5000.0$ and $k = 0.25$. It is consistent with a power-law form $P(v) \sim v^{-\gamma}$, where $v > 0$ and $\gamma \approx 2.5$, in agreement with the value reported in Ref. [30] and the deviation observed can be attributed to the finite height of well. On the other hand, averaged Floquet state in the KR limit for $V_0 = 0.5$ and $k = 0.25$ shown in Fig. 2(b) displays exponential decay, $P(v) \sim \exp(-v/l)$, where l is the localization length. This is the standard dynamical localization scenario but is generally not associated with non-KAM systems. Both these decay profiles in Fig. 2 can be understood if the relation between singular potential and power-law localization can be restated in the following manner. For this purpose, let $\epsilon_{if} = \{E_i, E_{i+1}, E_{i+2}, \ldots E_f\}$ collectively represent the energies of a set of states of H_0 lying in the energy band $(E_f - E_i)$ between two states with quantum numbers f and i in the unperturbed system. The classical singularities are associated with quantum power-law localization of a set of Floquet states mostly lying in the energy range ϵ_{if}, provided $\epsilon_{if} < V_0$. Thus, Floquet states will display power-law localization only if they effectively "feel" the non-smooth potential. This requires that energy scale ϵ_{if} be less than that of V_0.

It must be emphasized that the Hamiltonian in Eq. (1) is classically a non-KAM system if $V_0 > 0$, for all values of $k > 0$. Hence, with $V_0 = 5000.0$ and for kick strength as small as $k = 0.25$ the system is classically chaotic (Appendix A) and the corresponding quantized system displays power-law localized profile of the Floquet states [Fig. 2(a)]. In this case, most of the 10035 Floquet states used for averaging are such that $\epsilon_{if} < V_0$. On the other hand, in the case of Fig. 2(b), even though it is still a non-KAM system with singular potential, the Floquet states mostly straddle energy scales ϵ_{if} larger than V_0 and are not affected by the shallow singular potential and hence the exponentially localized Floquet states are obtained.

A. Matrix element decay

It is known that exponential localization in the KR is associated with the exponential decay of the matrix elements of the corresponding Floquet operator. Further, from Refs. [29,30], it is also known that in the case of KR in the infinite well, a non-KAM system, the matrix elements of $\widehat{U}$ display a power-law decay after a bandwidth $\eta \propto k$. Hence, it is natural to enquire how the decay of matrix elements changes its character

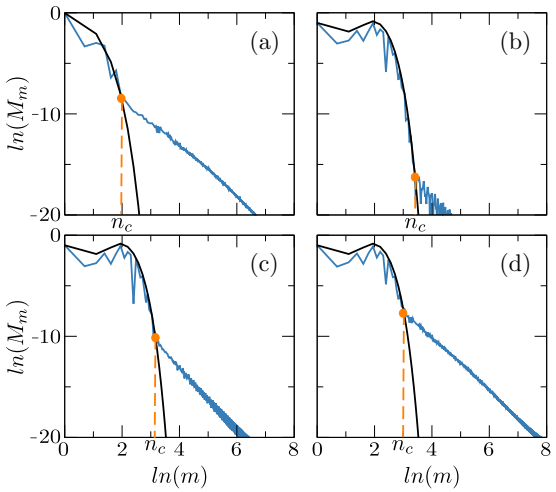

FIG. 3. Averaged decay of the matrix elements of the Floquet operator $\widehat{U}$ as a function of m. The parameters are $b = 1.4\pi, \hbar_s = 1.0$, (a) (KRIW limit) $V_0 = 5000.0, k = 0.25$, and (b) (KR limit) $V_0 = 0.5, k = 4.25$, (c) $V_0 = 100.0, k = 4.25$, (d) $V_0 = 5000.0, k = 4.25$. n_c represents the crossover point from exponential to power-law profile. All black curves corresponds to KR.

as $V_0 \gg 1$ approaches the limit $V_0 \to 0$. In the unperturbed basis, the matrix elements are U_{nm} as given by Eq. (4). This is illustrated in Fig. 3, which shows $M_m = \langle |U_{nm}| \rangle_n$ as a function of m, with $m > n$, in log-log plot.

Figures 3(a) and 3(b) show M_n as log-log plot for the same choice of parameters as in Figs. 2(a) and 2(b). Figure 3(a) corresponds to KRIW limit and shows a short regime of exponential decay followed by an asymptotic power-law decay. In Fig. 3(b), $V_0 = 0.5$ corresponding to the KR limit and the decay of M_n largely follows that of KR except for $n \gg 1$ where it decays as a power-law. In general, the following features are observed. In the limit as $V_0 \to \infty$, the decay is of power-law form. In the opposite limit of $V_0 \to 0$, the decay is exponential in nature. In general, for any intermediate V_0, i.e., $0 < V_0 < \infty$, an initial exponential decay is followed by an asymptotic power-law decay whose slope is approximately 2.7. If $V_0 < \infty$, the initial exponential decay is always present. The exponential decay sharply changes over to a power-law decay at $n = n_c$ as shown by dotted vertical lines in Fig. 3. For any fixed value of kick strength k, as V_0 varies from $0 \to \infty$, then n_c changes from $\infty \to 0$. It is also to be noted that for fixed V_0, as k increases, n_c also increases.

B. Energy scales

In this section, we show how singularity of the potential and energy scales associated with the Floquet states determine the localization structure of these states. As discussed in Sec. II, $c_{rj} = \langle \phi_r | \psi_j \rangle$, where $|\psi_j\rangle$ is an eigenstate of H_0 with associated energy E_j. Let $c_{\max} = \max(|c_{r,1}|^2, |c_{r,2}|^2, \ldots |c_{r,N}|^2)$ represent the largest overlap of rth Floquet state with $|\psi_j\rangle$. The energy associated with $|\psi_j\rangle$, and hence with $c_{\max}$, is denoted by $E_{\max}$. Then, an effective parameter $\mu = E_{\max}/V_0$ can be identified to distinguish two regimes, namely, (i) $\mu \leqslant 1$ and (ii) $\mu \gg 1$. Physically, $\mu \leqslant 1$ corresponds to Floquet states (in energy basis) mostly confined to the potential height V_0 and

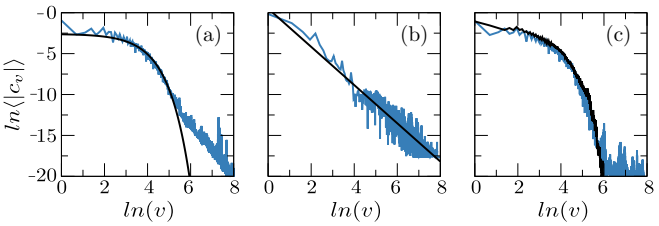

FIG. 4. Floquet states of Hamiltonian in Eq. (1) with parameters $b = 1.4\pi, \hbar_s = 1.0, V_0 = 5000.0, k = 4.25$. The three figures differ in how Floquet states were averaged over: (a) averaged over all the computed states, (b) averaged over states with $\mu < 1$, (c) averaged over states with $\mu \gg 1$. In (a, b) the black curve represents best fit line, and in (c) the black curve corresponds to KR.

$\mu \gg 1$ corresponds to those Floquet states that have significant overlap with states lying in the energy scales far greater than V_0.

In Fig. 4(a), $\ln\langle c_v \rangle$ is shown by averaging over all the computed Floquet states for $V_0 = 5000.0$ and $k = 4.25$. As discussed earlier, the Floquet state profile is a combination of initial exponential decay followed by a power-law decay. However, if average is taken only over those states that satisfy the condition $\mu \leqslant 1$, then the resulting profile is shown in Fig. 4(b). In this case, $k = 4.25$ and all the Floquet states are confined to an energy scale well below V_0. Hence, this set of Floquet states can be expected to "feel" the presence of singularity in the potential. In this regime, we observe a power-law profile for the averaged Floquet states as displayed in Fig. 4(b). Based on the results of earlier works [2], this set of states can be expected to display multifractal properties as well.

However, if the states are averaged subject to the condition that $\mu \gg 1$, then singularity is not strongly felt by the Floquet states since the bandwidth of their energy distribution is far greater than V_0. Effectively, at this energy scale, the singularity becomes insignificant and hence we can expect it to lie in the KR limit. Indeed, as seen in Fig. 4(c), $\langle c_v \rangle$ is nearly identical to that of KR [shown as black curve in Fig. 4(c)] at $k = 4.25$.

In general, for the Hamiltonian in Eq. (1), the localization property of a subset of Floquet states in an energy band ϵ_{if} depends on the effectiveness of the singularity for the spectral range ϵ_{if} under consideration. In a given energy band ϵ_{if}, if the singularity is effective, then power-law localization is obtained and if singularity is weak or absent then exponential localization results for the states in ϵ_{if}. As far as localization of eigenstates of chaotic systems are concerned, it is known that either all the states are exponentially localized (as in KR) or power-law localized (as in systems with singular potentials) but, to the best of our knowledge, combinations of these localization profiles have not been reported before. In the next section, we transform the Hamiltonian in Eq. (1) to that of a tight-binding model and show that V_0/E controls the localization property of eigenvectors.

IV. TIGHT-BINDING MODEL

The dynamical localization in the quantum KR system was mapped to Anderson model for electron transport in a one-dimensional crystalline lattice [15]. By implication, the

exponential decay profile of eigenstates in the Anderson model translates to exponential profile (in the momentum representation) for the Floquet states of quantum KR. Following this mapping technique, in this section, we map the Hamiltonian in Eq. (1) to a tight-binding Hamiltonian. Since Eq. (1) represents a time periodic system, using Floquet-Bloch theorem, we can write the quasienergy state as

$$\phi(\theta,t) = e^{-i\omega t}u(\theta,t), \tag{5}$$

where, $u(\theta,t) = u(\theta,t+1)$. In between two consecutive kicks, the Hamiltonian H_0 governs the evolution of the particle and is given by

$$\phi_n^-(t+1) = e^{-iE_n}\phi_n^+(t). \tag{6}$$

In this, $\phi_n^-(t+1)$ and $\phi_n^+(t)$ are the quasienergy states just before the $(t+1)$th kick and just after tth kick and E_n is the nth energy level of H_0. During the evolution it acquires an extra phase e^{-iE_n}. By substituting Eq. (5) in Eq. (6) and using the periodicity of $u(\theta,t)$, we obtain

$$u_n^-(\theta,t+1) = e^{i\omega}e^{-iE_n}u_n^+(\theta,t). \tag{7}$$

Now the quasienergy state just after a tth kick can be obtained using a map $\phi^+(\theta,t) = e^{-iV(\theta)}\phi^-(\theta,t)$. By using Eq. (5), this can be written in-terms of $u(\theta,t)$ as

$$u^+(\theta,t) = e^{-iV(\theta)}u^-(\theta,t). \tag{8}$$

Now, $e^{-iV(\theta)}$ is expressed in terms of trigonometric function $W(\theta) = -\tan(\frac{V(\theta)}{2})$ as

$$e^{-iV(\theta)} = \frac{1+iW(\theta)}{1-iW(\theta)}. \tag{9}$$

This is used in Eq. (8) to obtain

$$\frac{u^+(\theta)}{1+iW(\theta)} = \bar{u} = \frac{u^-(\theta)}{1-iW(\theta)}, \tag{10}$$

where $\bar{u}$ is defined as $\bar{u} = [u^+(\theta)+u^-(\theta)]/2$. Using Eqs. (8) and (9), the evolution of the quasienergy state after one period is

$$u^+(\theta) = e^{-iV(\theta)}e^{i(\omega-E_n)}u^+(\theta). \tag{11}$$

This can be written as

$$[1-iW(\theta)]\bar{u} = e^{i(\omega-H_0)}\bar{u}[1+iW(\theta)], \tag{12}$$

where $\bar{u} = \frac{u^+}{1+iW(\theta)}$. Now rearrangement of terms leads to

$$\tan\left(\frac{\omega-H_0}{2}\right)\bar{u} + W(\theta)\bar{u} = 0. \tag{13}$$

The quasienergy state can be expanded in the unperturbed basis as $|\bar{u}\rangle = \sum_m u_m|\psi_m\rangle$, where $|\psi_m\rangle$ are the eigenstates of H_0 and u_m is given by

$$u_m = \int \bar{u}\psi_m(\theta)d\theta = \int \frac{1}{2}[u^+(\theta)+u^-(\theta)]\psi_m(\theta)d\theta. \tag{14}$$

Taking the inner product of Eq. (13) with $|\psi_m\rangle$, we will formally obtain

$$T_m u_m + \sum_l W_{ml}u_l = 0. \tag{15}$$

In this, $T_m = \tan(\frac{\omega-E_m}{2})$ represents the on-site energy and W_{ml} is the hopping strength for a particle to hop from mth site to lth site and can be written in the energy basis as

$$\begin{aligned} W_{ml} &= \langle\psi_m|W(\theta)|\psi_l\rangle \\ &= \int \sum_{p,q} a_{mp}^* e^{-ip\theta}W(\theta)a_{lq}e^{iq\theta}d\theta \\ &= \sum_{p,q} a_{mp}^* a_{lq}\int W(\theta)e^{-i(p-q)\theta}d\theta \\ &= \sum_{p,q} a_{mp}^* a_{lq}W_{p-q}, \end{aligned} \tag{16}$$

where $W_n = \frac{1}{2\pi}\int_0^{2\pi} W(\theta)e^{-in\theta}d\theta$ is the Fourier transform of $W(\theta)$. Thus, in energy basis, after simple manipulation, Eq. (15) takes the form

$$\left(T_m + \sum_{p,q} a_{mp}^* a_{mq}W_{p-q}\right)u_m + \sum_{p,q,l\neq m} a_{mp}^* a_{lq}W_{p-q}u_l = 0. \tag{17}$$

This is the tight-binding model version of the Hamiltonian in Eq. (1). In this, $(T_m + \sum_{p,q} a_{mp}^* a_{mq}W_{p-q})$ represents the diagonal term and $a_{mp}^* a_{lq}W_{p-q}$ is the off-diagonal term of the transfer matrix. It does not appear straightforward to analytically prove power-law profile of Floquet states starting from Eq. (17), though it appears fair to expect that in this case the decay of Floquet state profile will be different from exponential form. As numerical results show, we obtain power-law localization. Similar results has also been reported in Ref. [38].

However, using Eq. (17), it is possible to make an inference about Floquet state profile in the limit $\mu \gg 1$. In this case, $E_n \gg V_0$ and the singularity in the potential becomes insignificant. Effectively, the system behaves as a free particle with energy $E_n = \frac{\hbar_s n^2}{2}$ and the wave function of H_0 is just the momentum eigenstate, $|\psi_n\rangle = a_{nn}e^{in\theta}$, with $a_{mn} = \delta_{mn}$. This set of conditions, if applied to Eq. (17), leads to

$$(T_m + W_0)u_m + \sum_l W_{m-l}u_l = 0. \tag{18}$$

This is just standard KR Hamiltonian transformed to the 1D Anderson model [15], for which all the eigenstates are known to display exponential profile. Hence, as seen in Fig. 4(c) for $\mu \gg 1$, the observed localization is exponential in nature. Thus, even in the presence of singular potentials, eigenstate localization is not generically of power-law form. We reiterate the main result of the paper that the association between power-law profile of eigenstates and singular potentials needs to take into account the effectiveness of singularity in a given energy band.

V. SPECTRAL SIGNATURES

Based on the results presented in Fig. 4, a novel scenario for the spectral signatures can be expected. As the regimes $\mu < 1$ and $\mu \gg 1$ are traversed, by considering Floquet states in a suitable energy band ϵ_{if}, the decay profile of Floquet state changes from power-law to exponential form. This would also

imply that a unique spectral signature for the nearest-neighbor spacing distribution $P(s)$, such as either the Poisson or Wigner distributions, may not exist for the system as a whole. Quite unusually, $P(s)$ would depend on the energy band ϵ_{if} being considered. Thus, in the same system for a given choice of parameters, in the limit $\mu \gg 1$ (KR limit) we expect Poisson distribution and in the limit $\mu < 1$ (KRIW limit) we expect $P(s)$ to display intermediate spacing statistics such as semi-Poisson distribution (see Appendix B).

The Floquet operator $\hat{U}$ being a unitary operator, all the eigenvalues lie on a unit circle, $\omega_i \in [0, 2\pi)$. In this case, level density is constant ($\frac{N}{2\pi}$) and hence the unfolding of Floquet levels is not necessary. To compute the spacing distribution, we have treated the eigenvalues of even and odd parity states separately. The nearest-neighbor spacing distribution reveals two different forms: for $\mu < 1$ level repulsion is observed in the form of semi-Poisson distribution and for $\mu \gg 1$ level clustering is seen in the form of Poisson distribution (Appendix B). The regime of $\mu < 1$ corresponds to KRIW limit and power-law decay of Floquet states [see Fig. 4(b)] and is associated with level correlations that are intermediate between no correlation and random matrix type level repulsion. Indeed, as shown in the spacings distributions in Appendix A, the level spacing statistics deviate from Wigner distribution and is consistent with the semi-Poisson distribution.

On the other hand, the limit of $\mu \gg 1$ is KR limit (potential singularity is ineffective) and levels remain uncorrelated due to occurrence of dynamical localization resulting in Poisson spacing distribution (see Appendix A). It must be emphasized that two different level spacing distributions and level correlations for the same system with identical parameters is a novel feature not usually encountered in the context of chaotic quantum systems. This unusual spacing distribution reinforces the central result of this paper that the relation between potential singularity and eigenvector profile is conditioned by energy regime being considered.

This dichotomy is reflected in the eigenvector statistics as well. This is easily observed by studying the participation ratio (PR) of the Floquet states that provides information about their localization properties. For an eigenstate that resides in the infinite dimensional Hilbert space, participation ratio is defined as

$$P = \sum_{i=1}^{\infty} |\psi_i|^4 \tag{19}$$

with the condition that $\sum_i |\psi_i|^2 = 1.0$, where ψ_i are components of a Floquet state. It is a measure of how many basis states effectively participate in making up the eigenstate. If $P \approx 1$, then the state is strongly localized and implies that one basis state contributes significantly to the Floquet state while the contribution from the rest of the basis are almost negligible. However, if $P \sim \frac{1}{N}$, then the Floquet state is of extended nature and all the basis states make equal contribution on an average. Figure 5 displays P for all the 10 035 converged Floquet states as a function of energy $E_{\max}$ for the identical choice of parameters as in Fig. 4. Quite surprisingly, P distinguishes the two regimes, $\mu < 1$ and $\mu \gg 1$. The boundary between the two regimes is at $E_{\max} = V_0$, the height of potential barriers. For $\mu \gg 1$, exponential localization of Floquet states implies that

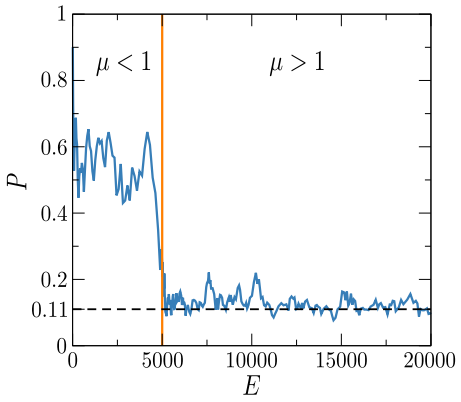

FIG. 5. Participation ratio of the Floquet states as a function of $E_{\max}$ for $b = 1.4\pi$, $\hbar_s = 1.0$, $V_0 = 5000.0$, $k = 4.25$ (same set of parameters as in Fig. 4). The vertical line is placed at $E_{\max} = V_0$ ($\mu = 1$), the height of potential barriers. Horizontal black dotted line represents the mean participation ratio for $\mu > 1$.

$|\phi\rangle \sim e^{-n/l}$, where l is the localization length. A remarkable result due to Izrailev [14,39] provides the relation, $l \approx \frac{k^2}{2\hbar_s^2}$. For our case, this estimate gives $l \approx \frac{k^2}{2\hbar_s^2} = 9.03$ and this represents the effective number of basis states that goes in constructing the Floquet states. As participation ratio is the inverse of the effective number of basis states, it is estimated to be $P \approx \frac{2\hbar_s^2}{k^2} = 0.11$. As seen in Fig. 5, this value closely matches the computed PR in the regime $\mu \gg 1$.

For $\mu < 1$, the mean P is larger compared to that for $\mu > 1$ as shown in Fig. 5. The reason can be traced back to the fact that in the case of infinite well $E_n \sim n^2$ and hence levels are spaced far apart. This implies that the Floquet states for $\mu < 1$ has overlap only with a few unperturbed basis states and this effectively increases the value of participation ratio for $\mu < 1$. Ultimately, this results in a more compact localization.

Finally, all the results discussed in this paper can be summarized in the form of a "phase diagram" displayed in Fig. 6. For $\mu < 1$, singularity in the potential is effective and

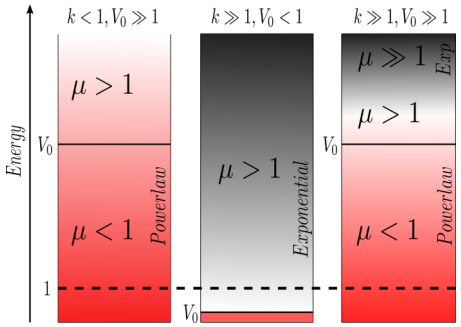

FIG. 6. Summary of the results presented in this work. In all the cases, the potential V_{sq} is singular. Power-law decay profile of the Floquet is obtained whenever $\mu < 1$ (shown as deep red). Stronger red color represents power-law profile over larger energy scales. For $\mu > 1$, exponential localization is obtained. Darker gray represents dominant exponential profile over longer energy scales. White color represents regimes of transition between these profiles. They cannot be classified as power law or exponential with definiteness.

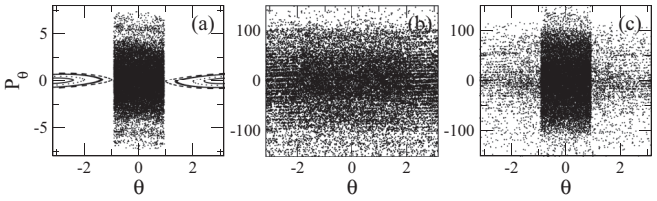

FIG. 7. Stroboscopic sections of kicked particles in a periodic square well potential for $b = 1.4\pi$, (a) $V_0 = 5000.0, k = 0.25$, (b) $V_0 = 0.5, k = 4.25$, and (c) $V_0 = 5000.0, k = 4.25$.

hence power-law profile of the Floquet states is obtained. This regime is indicated by red color in Fig. 6. However, if $\mu > 1$, singularity is not effectively "felt" by the particle, and hence exponential profile is obtained. This regime is indicated by black color in the figure. Depending on the choice of parameters, regimes in which transition occurs between these two Floquet state profiles are also observed. In Fig. 6, this is indicated by white color.

VI. CONCLUSION

In summary, we have studied a non-KAM system represented by the Hamiltonian in Eq. (1), namely a periodically kicked particle in a finite potential well of height V_0, to primarily understand the nature of its Floquet states. This Hamiltonian can be thought of as representing two limiting cases: (i) the standard KR for $V_0 = 0$ and (ii) KR in infinite potential well for $V_0 \to \infty$. It is well known that, for sufficiently large kick strengths, all the Floquet states of the KR are localized with an exponential profile [14]. Further, it has been suggested that for kicked systems with singularity in their potential, the Floquet states display power-law profile [31]. We examine the Floquet states of the Hamiltonian in Eq. (1) in the light of these results. To understand its Floquet states, we map this problem to that of a tight-binding model.

The results presented in this work show that the decay profile of the Floquet states is not determined by the potential singularity alone, but by the representative energy band ϵ_{if} of a set of Floquet states relative to the potential height V_0. Thus, we show that if $\epsilon_{if} > V_0$ then the effect of singularity is weak for the set of Floquet states, and they display exponential profile. This represents the KR limit of the problem. On the other hand, the condition $V_0 > \epsilon_{if}$ represents Floquet states strongly affected by the singular potential. In this case, we have shown that Floquet states have predominantly power-law profile. This is also the regime in which the eigenfunctions can be expected to display multifractality [2]. We note that the system presented in this work resides in infinite-dimensional Hilbert space, which makes it particularly not a straightforward exercise to interpret multifractal measures such as singularity spectrum and multifractal dimensions.

In the regime intermediate between the extremes of KR and KRIW, the Floquet states typically display an initial exponential decay followed by an asymptotic power-law decay. The presence of these two contrasting Floquet state profiles in Hamiltonian in Eq. (1) leaves its signature in the spectral correlations as well. For an identically same set of parameters, depending on the reference energy scale ϵ_{if}, the spacing distribution turns out to be Poisson distribution ($\epsilon_{if} > V_0$) or

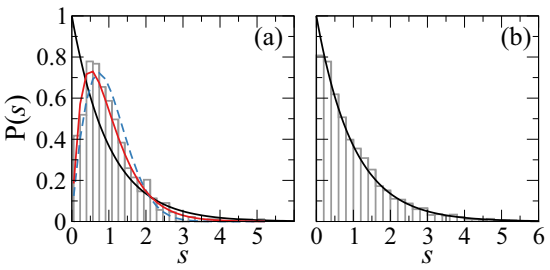

FIG. 8. Numerically computed spacing distribution (histograms) $P(s)$ for $b = 1.4\pi, k = 4.25, V_0 = 1\,500\,000.0$ and $\hbar_s = 1.0$, (a) $\mu < 1$, (b) $\mu \gg 1$. Solid black line represents Poisson distribution, dashed (blue) line represents Wigner distribution, and solid (red) line represents semi-Poisson distribution.

a semi-Poisson distribution ($V_0 > \epsilon_{if}$). Typically, the spacing distribution is taken to characterize quantum chaos in a system and it is generally independent of the energy band being considered provided it is in the semiclassical limit. Quite surprisingly, the semiclassical limit of the system in Eq. (1) lacks a unique spacing distribution as it depends on the energy band ϵ_{if} being considered. KR was experimentally realized in a test-bed of cold atomic cloud in flashing optical lattices. Using more than one optical lattice, KR confined to a "potential well" has also been realized. We believe that the results in this work are amenable to experiments in a suitable atom-optics set up.

ACKNOWLEDGMENT

S.P. acknowledges the University Grants Commission of India for research fellowship.

APPENDIX A: STROBOSCOPIC SECTION

In this work, a periodically kicked particle in a periodic potential well [Eq. (1)] is studied. Figure 7 shows the classical stroboscopic section corresponding to the parameters used in Figs. 2 and 4. For the choice of parameters used in this work, the system is classically chaotic as seen in Fig. 7. The sections were computed using the map described in Ref. [36].

APPENDIX B: SPACING DISTRIBUTION

In Fig. 8 we show the level spacing distribution for the following cases: (a) $\mu < 1$ (KRIW limit) and (b) $\mu \gg 1$ (KR limit).

We have used a large value of V_0 to obtain a sufficient number of symmetry decomposed Floquet eigenvalues in the $\mu < 1$ regime to calculate the spacing distribution. This figure demonstrates that the spacing distribution for $\mu < 1$ deviates from Wigner distribution and is consistent with semi-Poisson distribution. This is to be expected based on earlier works [33] that have shown that Hamiltonians with singular potentials, in certain parametric regimes, display intermediate statistics such as the semi-Poisson distribution. On the other hand, the spacing distribution in the $\mu \gg 1$ regime follows Poisson distribution which implies uncorrelated eigenvalues. The eigenfunctions display localization and are similar to the eigenfunctions of KR system.

[1] J. Chabe, G. Lemarie, B. Gremaud, D. Delande, P. Szriftgiser, and J. C. Garreau, Phys. Rev. Lett. **101**, 255702 (2008); J. Wang, C. Tian, and A. Altland, Phys. Rev. B **89**, 195105 (2014).

[2] A. M. Garcia-Garcia and J. Wang, Phys. Rev. Lett. **94**, 244102 (2005); Acta Phys. Pol. A **112**, 635 (2007).

[3] J. Gong and P. Brumer, Phys. Rev. Lett. **86**, 1741 (2001); J. Gong, H. J. Worner, and P. Brumer, Phys. Rev. E **68**, 056202 (2003).

[4] F. Matsui, H. S. Yamada, and K. S. Ikeda, Europhys. Lett. **114**, 60010 (2016); A. Lakshminarayan, Phys. Rev. E **64**, 036207 (2001); P. A. Miller and S. Sarkar, Nonlinearity **12**, 419 (1999); M. S. Santhanam, V. B. Sheorey, and A. Lakshminarayan, Phys. Rev. E **77**, 026213 (2008).

[5] S. Fishman, I. Guarneri, and L. Rebuzzini, Phys. Rev. Lett. **89**, 084101 (2002).

[6] M. Lepers, V. Zehnle, and J. C. Garreau, Phys. Rev. A **77**, 043628 (2008).

[7] G. Behinaein, V. Ramareddy, P. Ahmadi, and G. S. Summy, Phys. Rev. Lett. **97**, 244101 (2006).

[8] I. Dana and D. L. Dorofeev, Phys. Rev. E **73**, 026206 (2006).

[9] H. Schanz, M.-F. Otto, R. Ketzmerick, and Th. Dittrich, Phys. Rev. Lett. **87**, 070601 (2001); P. H. Jones, M. Goonasekera, and F. Renzoni, *ibid.* **93**, 073904 (2004); T. S. Monteiro, P. A. Dando, N. A. C. Hutchings, and M. R. Isherwood, *ibid.* **89**, 194102 (2002).

[10] I. Dana, V. Ramareddy, I. Talukdar, and G. S. Summy, Phys. Rev. Lett. **100**, 024103 (2008).

[11] P. H. Jones, M. M. Stocklin, G. Hur, and T. S. Monteiro, Phys. Rev. Lett. **93**, 223002 (2004); P. H. Jones, M. Goonasekera, D. R. Meacher, T. Jonckheere, and T. S. Monteiro, *ibid.* **98**, 073002 (2007); M. Sadgrove, S. Wimberger, S. Parkins, and R. Leonhardt, *ibid.* **94**, 174103 (2005).

[12] S. Sarkar, S. Paul, C. Vishwakarma, S. Kumar, G. Verma, M. Sainath, U. D. Rapol, and M. S. Santhanam, Phys. Rev. Lett. **118**, 174101 (2017); B. G. Klappauf, W. H. Oskay, D. A. Steck, and M. G. Raizen, *ibid.* **81**, 1203 (1998).

[13] H. Schomerus and E. Lutz, Phys. Rev. Lett. **98**, 260401 (2007); Phys. Rev. A **77**, 062113 (2008).

[14] F. M. Izrailev, Phys. Rep. **196**, 299 (1990).

[15] S. Fishman, D. R. Grempel, and R. E. Prange, Phys. Rev. Lett. **49**, 509 (1982); D. R. Grempel, R. E. Prange, and S. Fishman, Phys. Rev. A **29**, 1639 (1984); S. Fishman, R. E. Prange, and M. Griniasty, *ibid.* **39**, 1628 (1989).

[16] H-J. Stockmann, *Quantum Chaos: An Introduction* (Cambridge University Press, Cambridge, 1999).

[17] L. Reichl, *The Transition to Chaos: Conservative Classical Systems and Quantum Manifestations* (Springer, Berlin, 2004).

[18] P. W. Anderson, Phys. Rev. **109**, 1492 (1958).

[19] *50 Years of Anderson Localization*, edited by E. Abrahams (World Scientific, Singapore, 2010).

[20] D. L. Shepelyansky, Phys. Rev. Lett. **56**, 677 (1986); Physica D **28**, 103 (1987).

[21] F. L. Moore, J. C. Robinson, C. Bharucha, P. E. Williams, and M. G. Raizen, Phys. Rev. Lett. **73**, 2974 (1994); F. L. Moore, J. C. Robinson, C. F. Bharucha, B. Sundaram, and M. G. Raizen, *ibid.* **75**, 4598 (1995).

[22] J. Ringot, P. Szriftgiser, J. C. Garreau, and D. Delande, Phys. Rev. Lett. **85**, 2741 (2000).

[23] T. M. Fromhold *et al.*, J. Opt. B: Quantum Semiclassical Opt. **2**, 628 (2000).

[24] M. Tabor, *Chaos and Integrability in Nonlinear Dynamics: An Introduction* (Wiley, New York, 1989); J. Poschel, Proc. Symposia Pure Math. **69**, 707 (2001); S. Wiggins, *Global Bifurcations and Chaos: Analytical Methods*, Vol. 73 (Springer Science and Business Media, Berlin, 2013).

[25] B. Sundaram and G. M. Zaslavsky, Phys. Rev. E **59**, 7231 (1999).

[26] I. Guarneri, G. Casati, and V. Karle, Phys. Rev. Lett. **113**, 174101 (2014).

[27] R. Dutta and P. Shukla, Phys. Rev. E **78**, 031115 (2008).

[28] B. G. Klappauf, W. H. Oskay, D. A. Steck, and M. G. Raizen, Phys. Rev. Lett. **81**, 4044 (1998).

[29] R. Sankaranarayanan, A. Lakshminarayan, and V. B. Sheorey, Phys. Rev. E **64**, 046210 (2001).

[30] B. Hu, B. Li, J. Liu, and Y. Gu, Phys. Rev. Lett. **82**, 4224 (1999).

[31] J. Liu, W. T. Cheng, and C. G. Cheng, Commun. Theor. Phys. **33**, 15–20 (2000).

[32] J. Wang and A. M. Garcia-Garcia, Phys. Rev. E **79**, 036206 (2009).

[33] A. M. Garcia-Garcia and J. Wang, Phys. Rev. E **73**, 036210 (2006).

[34] A. M. Garcia-Garcia, Phys. Rev. E **72**, 066210 (2005).

[35] J. Martin, I. Garcia-Mata, O. Giraud, and B. Georgeot, Phys. Rev. E **82**, 046206 (2010).

[36] S. Paul, H. Pal, and M. S. Santhanam, Phys. Rev. E **93**, 060203(R) (2016); H. Pal and M. S. Santhanam, *ibid.* **82**, 056212 (2010).

[37] J. V. Jose and R. Cordery, Phys. Rev. Lett. **56**, 290 (1986).

[38] A. Cohen and S. Fishman, Int. J. Mod. Phys. B **02**, 103 (1988).

[39] B. V. Chirikov, F. M. Izrailev, and D. L. Shepelyansky, Sov. Sci. Rev. C **2**, 209 (1981).